

N³: Addressing and Routing in 3D Nanonetworks

Ageliki Tsioliariidou¹, Christos Liaskos¹, Lefteris Pachis¹, Sotiris Ioannidis¹ and Andreas Pitsillides²

¹Foundation of Research and Technology - Hellas (FORTH), emails: {atsiolia,cliaskos,pachis,sotiris}@ics.forth.gr

²University of Cyprus, email: andreas.pitsillides@ucy.ac.cy

Abstract—Wireless communication at nanoscale faces unique challenges stemming from low hardware capabilities, limited power supply and unreliable channel conditions. The present paper proposes a networking scheme that can operate efficiently under such physical restrictions. Studying 3D multi-hop networks, the novel scheme offers scalable, trilateration-based node addressing and low-complexity packet routing mechanisms. Analysis is employed to design a routing process that balances path multiplicity for robust data delivery, and minimization of redundant transmissions. Extensive simulations yield increased resilience to challenging network conditions.¹

Index Terms—nanonetworks, 3D, addressing, routing, multi-hop.

I. INTRODUCTION

Nanonetworks comprise numerous wireless nodes manufactured at the scale of nm - μm . These miniaturized, communicating components allow for novel, groundbreaking products. For instance, smart materials can sense their environmental conditions, and change their internal structure to yield a programmatically defined end-behavior. Particularly, novel artificial materials have been proposed, which can receive external commands and alter their electromagnetic behavior (cf. software defined materials-SDMs [1]). Such components are expected to extend the reach of programmable (software-defined) networks to the level of material properties. For example, SDMs can be programmed to serve as perfect absorbers or reflectors of electromagnetic energy and light, maximizing the efficiency of renewable energy sources.

The architecture of nanonodes poses several restrictions at physical layer and, subsequently, to the networking layer as well. Firstly, the currently studied options for the power supply unit of each node are based on energy-harvesting, which allows for a very low uptime-to-downtime ratio [2]. Secondly, manufacturing scale and monetary cost considerations yield very limited processing capabilities per node [3]. Finally, considered choices for the communication spectrum (THz), coupled with the “weak” node hardware, yield unstable wireless channel conditions [4].

Compensating for these restrictions, related approaches at network layer assume a large communication radius per node, enough to contain the complete network. Thus, all communications are accomplished in one hop. In this manner, the data routing problem becomes a simple case of medium access control (MAC) [5]. Node addressing and location discovery is

¹This work was partially supported by the EU Horizon 2020 VirtuWind project (Grant no. 671648).

another major and open issue, due the described limitations. A common resolution is to assume networks with few nodes, each with a hard-coded, unique address [6]. Nonetheless, not all nanonetworking applications are compatible with these assumptions. Smart materials, for instance, can require thousands of nanonodes. Moreover, inter-node communication must be attained with very low power (and connectivity radius), to avoid interfering with the behavior of the material as a whole. Thus, packets reach their destination in multiple hops, requiring a data routing scheme [1].

The present paper contributes a node addressing and data routing scheme for multi-hop, peer-to-peer networks comprising a high number of static nodes. The addressing requires minimal overhead and is based on node trilateration. Thus, each node also acquires knowledge of its position in the network. A low-overhead routing process is proposed on top of the addressing system. It defines a geometric volume within the network space that contains the communicating node pair. Any other node contained within the volume acts as a retransmitter. The containment decision is taken with local information only, without input from neighboring nodes. The proposed scheme is supported analytically, and evaluated in terms of resilience to node failures and reduction of redundant transmissions.

II. RELATED WORK

Studies on nanonetworking have so far focused on physical-layer specifications (PHY), and compliant MAC.

PHY layer. Regarding channel models and nanoantennas, studies show operation at the THz band is promising due to antenna miniaturization potential [4]. Notice that THz communications are especially challenging due potent channel fading phenomena attributed to molecular absorption. The modulation and encoding scheme commonly follows the Rate Division Time Spread On-Off Keying (RD TS-OOK). Nanonodes transmit a logical “1” as a pulse and a logical “0” as silence. Finally, the nanonode power supply can be based on energy scavenging. This approach is based on piezoelectric nanogenerators which can produce enough energy for 1 packet transmission per roughly 10 sec [2].

MAC Layer. Studies have mainly focused on sparse, full-mesh topologies (i.e., one-hop), targeting Body Area Network (BAN) applications [6]. These studies assume hierarchical networks, where a set of sizable, relatively powerful nanorouters control the smaller, cheaper nanonodes. Nonetheless,

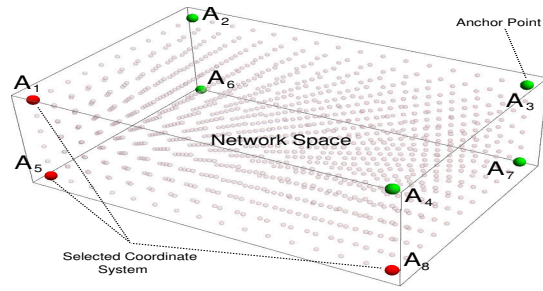


Figure 1. Overview of the studied nanonetwork.

this approach disrupts the unobtrusive advantage of nanonetworks. PHLAME is a distributed MAC protocol, which allows a transmitter and a receiver pair to choose the optimal communication parameters on demand, through a handshaking process [4]. The Division Time-Spread On-Off Keying modulation is used. The Receiver Initiated Harvesting-aware MAC protocol assumes that properly powered nodes advertise their retransmission capability, triggering data dissemination [5]. Both PHLAME and RIH-MAC are built on energy scavenging, thus being applicable to ultra-low network traffic cases. Conceptual similarities also exist among the studied nanonetworks and ad hoc networks-on-chips (NoCs) or macro-scale Wireless Sensor Networks (WSNs) [3]. Nonetheless, NoCs and WSNs assume much more powerful nodes than nanonetworks and very different wireless channel conditions [7]. Therefore, WSN and NoC-oriented solutions are generally not portable to nanonetworks.

Regarding our prior work, the authors presented and evaluated a ray-tracing-based simulation technique for nanonetworks in [8]. A flood-based data dissemination scheme for nanonetworks was proposed in [9], without solving the addressing problem. The scheme was then refined in terms of complexity [10]. A peer-to-peer routing and addressing scheme suitable only for simplified, 2D networks was proposed in [11]. Concerning *differentiation*, the present paper studies addressing and peer-to-peer routing in the realistic case of 3D networks, which are vital for nanonetworking applications such as smart materials.

III. OVERVIEW OF THE PROPOSED SCHEME

The proposed N^3 system assumes a set of nanonodes placed within a 3D rectangular *network space*, as shown in Fig. 1. The nodes can be placed randomly or by a uniform pattern within the space. This setup corresponds to material monitoring and active meta-materials applications, with a great number of nodes dispersed within the volume of the material [1]. All nodes are identical in terms of hardware, and have the same, short wireless connectivity radius. Thus, a packet is expected to reach its destination after many hops in general. Furthermore, we assume conditions operational conditions where node failures are common and, therefore, routing path redundancy is required. Nodes may temporarily fail for any spontaneous reason attributed to weak hardware or channel conditions. Furthermore, the low efficiency of

presently available options for node power supply means that few nodes are capable of wireless transmission at any given moment [4]. The high path redundancy and the multi-hop packet propagation yields increased packet transmissions at network level. Thus, minimizing the overhead information per each transmission is a top priority for N^3 .

Eight nanonodes, called *anchors*, are placed at the vertexes of the space during the construction of the material and are given indexes $A_1 \dots A_8$. The anchors are identical to any other node but have a unique role in the node *addressing* phase.

Node addressing. This phase occurs once and serves as the initialization of the network. It assigns addresses to the nanonodes, which are preserved for the lifetime of the material. The N^3 system uses the 3D location of a node as its address. Generally, a point in 3D space is uniquely identified by its distances from 4 other points. However, N^3 employs the distances from just three anchors, thus minimizing the overhead information as mentioned above. Moreover, the proper selection of three anchors out of the total eight can minimize redundant retransmissions. The analytical support for these issues is supplied in Section IV. In this Section we focus on the N^3 workflow only.

At first, all nodes are informed of their distances from the anchors as follows. The addressing phase starts with anchor A_1 broadcasting a data packet with the following structure:

setup flag (1 bit)	anchor index (3 bits)	hop count (var)
--------------------	-----------------------	-----------------

The *setup flag* is set to 1 to designate the initialization phase. The *anchor index* is set to 1 (for A_1) and the *hop count* to 1. Each recipient node discards the packet if another setup packet from $A_{anchor\ index}$ has been received. Else, the node: i) memorizes the hop count as its distance from anchor $A_{anchor\ index}$, ii) increases the hop count field by +1, and iii) broadcasts the packet. Upon reception of such a packet, the anchor with index (*anchor index*) + 1 (e.g., A_2) understands that it is its turn to generate a setup packet, allowing first for a trivial timeout to ensure the completion of the propagation in progress. Thus, at the end of the initialization phase each node has deduced its address as the hop distances, $\{r_i, i = 1 \dots 8\}$, from the anchors $A_1 \dots A_8$. Notice that several neighboring nodes are assigned the same address, i.e., an address refers to an *area* rather than a node. The network then enters its operational phase, described next.

Packet routing. N^3 defines a way for routing a packet from any sender node P_1 to any recipient P_2 , both identified by their addresses. The sender selects the indexes of *three* anchors, $\{\dot{A}, \ddot{A}, \ddot{\ddot{A}}\}$, out of $A_1 \dots A_8$ to serve as the *coordinate system (CS)* for the packet delivery towards P_2 . The selection process is the objective of the analysis (Section IV). The corresponding *usable addresses (UA)* of P_1 and P_2 are denoted as: $UA_1 : \{\dot{r}_1, \ddot{r}_1, \ddot{\ddot{r}}_1\}$ and $UA_2 : \{\dot{r}_2, \ddot{r}_2, \ddot{\ddot{r}}_2\}$. The sender then creates a packet structured as:

setup flag (1 bit)	Packet id (8 bits)	CS (3×3bits)
UA_1 (var)	UA_2 (var)	DATA (var)

where *packet id* is random integer and *DATA* is the payload of the packet. Any recipient node P then first checks if a packet with the same id has been already received, at which case it

discards the packet. Else, the node: i) memorizes the packet id for a trivial amount of time, in order to avoid route loops. ii) Deduces its usable address, $UA : \{\dot{r}, \ddot{r}, \ddot{\ddot{r}}\}$, based on the CS field. iii) Re-transmits the packet on the condition:

$$\begin{aligned} \min \{\dot{r}_1, \dot{r}_2\} \leq \dot{r} \leq \max \{\dot{r}_1, \dot{r}_2\} \text{ AND} \\ \min \{\ddot{r}_1, \ddot{r}_2\} \leq \ddot{r} \leq \max \{\ddot{r}_1, \ddot{r}_2\} \text{ AND} \\ \min \{\ddot{\ddot{r}}_1, \ddot{\ddot{r}}_2\} \leq \ddot{\ddot{r}} \leq \max \{\ddot{\ddot{r}}_1, \ddot{\ddot{r}}_2\} \quad (1) \end{aligned}$$

N^3 naturally balances path redundancy and energy efficiency concerns. First, it ensures that the network remains connected despite the adverse conditions, by assigning the same address to several neighboring nodes. Moreover, several alternative paths are defined by condition (1), which yields a volume containing P_1 and P_2 . (Specifically, the condition defines a volume of six intersecting spheres, one for each upper/lower bound of \dot{r} , \ddot{r} and $\ddot{\ddot{r}}$). However, this volume is generally a fraction of the total space, limiting the energy expended for wireless transmissions at network-wide level.

Notably, N^3 incurs a particularly small network overhead, since it does not require a node neighborhood discovery processes. In addition, it takes the weak node hardware into consideration, operating without routing tables (no memory overhead) and requiring simple integer calculations for its core operation (cond. (1)). Thus, the CPU architecture can be simplified considerably.

IV. ANALYSIS

This Section supports and optimizes the addressing and routing processes of N^3 . Specifically, it will be shown that: i) Three anchors suffice to identify a point within the 3D space, provided that they are located at the vertexes of the same face of the space, and ii) There always exist a path connecting any two nodes within the network, assuming retransmission based on the condition (1). Finally, we will proceed to optimize the sender's coordinate system selection, seeking to minimize the number of the ensuing retransmitting nodes.

Analytical support of N^3 . We seek to ensure there do not exist separated areas within the network space that share the same address. This can be shown by converting anchor distances to *unique* Cartesian coordinates.

Assume that the network space has side lengths X, Y, Z , and a Cartesian system, with $x \in [0, X], y \in [0, Y], z \in [0, Z]$. Let three anchors:

$$\dot{A} = \{0, 0, 0\}, \ddot{A} = \{X, 0, 0\}, \ddot{\ddot{A}} = \{0, 0, Z\} \quad (2)$$

Notice that, by proper rotation and transfer, these anchors can represent any triplet of vertexes on the same face of the 3D space. Furthermore, let any point within the space with Cartesian coordinates, $\{x, y, z\}$, and distances from the anchors, $\{\dot{r}, \ddot{r}, \ddot{\ddot{r}}\}$.

Lemma 1. *The Cartesian coordinates, $\{x, y, z\}$ can be uniquely derived from three anchor distances, $\{\dot{r}, \ddot{r}, \ddot{\ddot{r}}\}$, provided that the three anchors are located on the same face of the rectangular network space.*

Proof: The distances define the equations:

$$z = \sqrt{\dot{r}^2 - x^2 - y^2} \quad (3)$$

$$z = \sqrt{\ddot{r}^2 - (x - X)^2 - y^2} \quad (4)$$

$$z = Z - \sqrt{\ddot{\ddot{r}}^2 - x^2 - y^2} \quad (5)$$

From (3) and (4) we easily derive x uniquely as:

$$x = \frac{\dot{r}^2 - \ddot{r}^2 + X^2}{2X} \quad (6)$$

z is also uniquely identified from (3) and (5) as:

$$z = \frac{\dot{r}^2 - \ddot{\ddot{r}}^2 + Z^2}{2Z} \quad (7)$$

Finally, from (3) we obtain two candidate y values as:

$$y = \pm \sqrt{\dot{r}^2 - x^2 - z^2} \quad (8)$$

However, our initial requirement is that $y \in [0, Y]$. Thus, the negative solution can be rejected, leading to the unique definition of the complete triplet, $\{x, y, z\}$, QED. ■

Using Lemma 1 it can be deduced that a minimum of three² anchors suffice for the operation of N^3 . The rectangular bounds are the enabling factor for this reduction (cf. equation (8)). This also enables N^3 to minimize the overhead information in the packet formats of Section III.

We proceed to prove that N^3 guarantees the existence of a path connecting any node pair P_1, P_2 . Via condition (1), N^3 defines a volume that contains all retransmitting nodes. The proof consists at showing that this volume is compound. Initially, notice that the volume surface is defined by several spherical surface segments. Then, we prove the following utility:

Lemma. *The routing of N^3 always contains paths that originate from any surface point, $P \neq P_2$, and strictly approach the destination P_2 , over two adjacent spherical segments.*

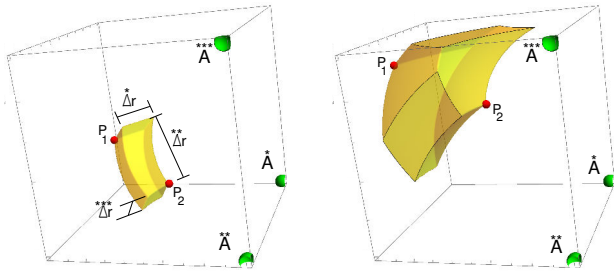
Proof: The proof is based on mathematical induction and is omitted. ■

Given the proven Lemma, we can show that N^3 always provides a path between any two nodes. Particularly, consider the following theoretical process:

- 1) Select and memorize a segment containing P_1 .
- 2) Move towards the destination over the selected segment. Stop if the destination has been reached.
- 3) At the points of discontinuities, select the adjacent segments unless previously memorized. Should the discontinuity refer to the intersection of the currently selected segment and the space boundaries, we move freely over the hit boundary towards the nearest spherical segments.
- 4) Memorize the selected segments.
- 5) For each selected segment, return to step 2.

According to the Lemma, the above process continuously reduces the distance to the destination, eventually reaching it. This concludes the proof that N^3 always offers a path connecting any node pair within a 3D rectangular space.

²Following the same steps, it can be shown that anchor triplets located on different faces of the network space do not have this property.



(a) Successful application of the $\prod \Delta r$ anchor selection approach. (b) The N^3 volume can be cropped by the space boundaries, invalidating the $\prod \Delta r$ approach.

Figure 2. Rationale and shortcomings of the $\prod \Delta r$ approach for coordinate system selection.

Optimization of N^3 . According to N^3 , the packet origin node, P_1 , is given the option to select the optimal coordinate system (anchor triplet) that will handle the complete packet propagation to P_2 . According to Lemma 1, there exist 24 valid coordinate system options (4 on each face of the space), denoted as the set \mathcal{CS} . Furthermore, each selection affects the number of retransmitters significantly [11], given that it alters the volume defined by condition (1). Therefore, we seek the optimal system, $cs_o \in \mathcal{CS}$, that minimizes the volume defined by condition (1). However, the analytical calculation of the volume is prohibitive for a hardware-constrained nano-node, even for three intersecting spheres [12]. Thus, we propose three heuristic approaches denoted as $\prod \Delta r$, $\sum \Delta r$ and Θ . Let $UA(P_1, cs) : \{\hat{r}_1, \check{r}_1, \ddot{r}_1\}$ and $UA(P_2, cs) : \{\hat{r}_2, \check{r}_2, \ddot{r}_2\}$ be the usable addresses of nodes P_1 and P_2 with regard to coordinate system $cs \in \mathcal{CS}$. Then, the optimal cs_o is selected as follows:

Approach 1 ($\prod \Delta r$).

$$cs_o \leftarrow \underset{cs \in \mathcal{CS}}{\operatorname{argmin}} \{ |\hat{r}_1 - \hat{r}_2| \cdot |\check{r}_1 - \check{r}_2| \cdot |\ddot{r}_1 - \ddot{r}_2| \}.$$

Approach 2 ($\sum \Delta r$).

$$cs_o \leftarrow \underset{cs \in \mathcal{CS}}{\operatorname{argmin}} \{ |\hat{r}_1 - \hat{r}_2| + |\check{r}_1 - \check{r}_2| + |\ddot{r}_1 - \ddot{r}_2| \}.$$

$\prod \Delta r$ approximates the volume of condition (1) by a 3D rectangle, as shown in Fig. 2a. The $\sum \Delta r$ is proposed as a computationally cheaper heuristic, given that it involves integer summations instead of multiplications. Both approaches require the original sender, P_1 , to check all valid cs options, i.e., incurring $O(24)$ complexity.

The $\prod \Delta r$ and $\sum \Delta r$ approaches may sufficiently approximate the volume of retransmitters, provided that the volume does not intersect with the space boundaries. Such a counterexample is shown in Fig. 2b, where the actual volume of retransmitters is much smaller than the approximated, due to the cropping at the space bounds.

We proceed to the Θ -approach that incorporates the essence of proximity to the space bounds as follows. Using the notation of Fig. 3 (top inset), we calculate the angle $\Theta = \angle P_1 A P_2$,

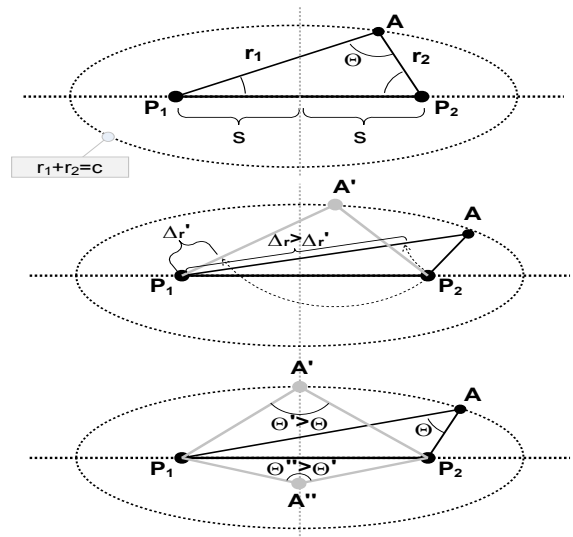


Figure 3. Qualitative relations between possible anchor positions and the Δr , Θ quantities.

defined by the communicating pair of nodes and any anchor A (omitting the proof):

$$\Theta = \operatorname{acos} \left(\frac{\Delta r \cdot c - 4s^2}{4s \cdot (c - \Delta r)} \right) - \operatorname{acos} \left(\frac{\Delta r \cdot c + 4s^2}{4s \cdot (c + \Delta r)} \right) \quad (9)$$

where $\Delta r = r_2 - r_1$, while $\Theta = \pi$ if $r_1 \cdot r_2 = 0$. Noticing the middle inset of Fig. 3, we observe that there exists a 1 – 1 monotonous relation between the angle Θ and Δr . Specifically, Δr decreases as Θ increases. In this aspect, the angle Θ incorporates the concern for small volume of retransmitters, given that Δr is a definitive factor, as illustrated in Fig. 2a. Moreover, the larger Θ angles are observed when the communicating points are close to the anchor and, therefore, in close proximity to the space bounds as well (cf. bottom inset of Fig. 3). Such volumes are most likely cropped by the bounds, limiting the number of contained retransmitters. With these observations in mind, the Θ approach for the selection of cs_o at the sender P_1 is defined as follows:

Approach 3 (Θ).

- 1) Set $s \approx \frac{1}{2} \cdot \max_{i=1 \dots 8} \{|r_1(A_i) - r_2(A_i)|\}$
- 2) Set $\hat{I} \leftarrow \underset{i=1 \dots 8}{\operatorname{argmin}} \{|r_1(A_i) - r_2(A_i)|\}$
- 3) Set $\check{I} \leftarrow \underset{i=1 \dots 8, \neq \hat{I}}{\operatorname{argmax}} \{\Theta | \Theta = \angle P_1 \widehat{A_i} P_2, \operatorname{face}(A_i, A_i)\}$
- 4) Set $\ddot{I} \leftarrow \underset{i=1 \dots 8, \neq \hat{I}, \check{I}}{\operatorname{argmax}} \{\Theta | \Theta = \angle P_1 \widehat{A_i} P_2, \operatorname{face}(A_i, A_i, A_i)\}$
- 5) Select $cs_o \leftarrow \{A_{\hat{I}}, A_{\check{I}}, A_{\ddot{I}}\}$

where $\operatorname{face}(\dots)$ is a binary predicate that yields true when the vertexes (\dots) are on the same face of the rectangular network space, complying with Lemma 1. Step 1 seeks to reduce computations by approximating the distance s between P_1 and P_2 as the maximum observed Δr over all anchors. Since all 8 anchors are iterated, we also select the first

optimal anchor as the one yielding the lowest Δr , cutting back calculations further (step 2). Steps 2-3 select the remaining two optimal anchors in accordance with the Θ angle as discussed. Notice that due to Lemma 1, the search of step 3 is restricted to 6 anchors only. For the same reason, step 4 is restricted to 4 or 2 anchors, depending on whether $A_j, A_{\bar{j}}$ are located on the same edge or not respectively. Thus, the complexity of the Θ approach is $O(16) - O(18)$. However, it requires capability for floating point operations, due to the form of equation (9).

Finally, notice that all proposed approaches have the advantage of operating without knowledge of the network space dimensions, contrary to exact analytical processes [12].

V. EVALUATION

This Section evaluates: i) the comparative performance of the coordinate system selection approaches, and ii) the resilience of N^3 against node failures, compared to the shortest path routing approach. The comparison metrics are the ratio of successful packet deliveries between random sender/receiver node pairs, and the number of involved retransmitters. The simulator is implemented on the AnyLogic platform [13], and the parameters are given in Table I.

System setup. Regarding topologies, three cases of 3D spaces are examined, each with a distinct ratio of dimensions (keeping the volume constant). Within each space, the nodes are placed on a regular grid. Each node is treated as a silicon cube (conductivity 0 S/m, permittivity 2.4 F/m) with a side of 10 μm . The space among the nodes is filled with air composed of standard atmospheric gases at normal humidity [14, p. 3 and p. 16]. The topology as a whole is intended to approximate a smart material application [1].

Regarding the channel model, the simulations use a full-3D ray tracing approach to deduce the propagation paths, their timing and attenuation [8]. All nodes are equipped with isotropic antennas. Molecular absorption due to the air (absorption coefficient K [15]) and shadow fading (X coefficient in dB [16]) are taken into account. The Signal to Interference plus Noise (SINR) model is used to deduce the success of a packet reception [17]. The transmission power was chosen to ensure that each node has ~ 20 neighbors within its connectivity radius which will be assigned the same N^3 address.

Evaluation of coordinate system selection. The simulation runs are configured as follows. The nodes are placed in each 3D space setup. To keep the runtimes tractable, only a subset of them (6^3 nodes, i.e., 6 equally-spaced nodes per grid dimension) are selected to serve as candidate senders/receivers. For each of the possible $\binom{6^3}{2}$ pairs, we execute a packet exchange and log the number of retransmitters yielded by each of the anchor selection approaches presented in Section IV. Additionally, we exhaustively check all valid coordinate systems (24) per pair, and deduce the one yielding the lowest number of transmitters in each case (*optimal*). All nodes are considered powered-on in this experiment. The results over all pairs are gathered in the form of boxplots, presented in Fig. 4.

Initially, it is observed that the space dimensions ratio plays a significant role to the average ratio of retransmitters

Table I
SIMULATION PARAMETERS

Parameter	Value
Communication & Power Parameters	
Frequency	100 GHz
Transmission Power	7dBmW
Noise Level	0dBmW
Reception SINR threshold	-10 dB
Guard Interval	0.1 nsec
Packet Duration	10nsec
Path Attenuation Parameters	
Absorption Coefficient K	0.52 dB/Km
Shadow Fading Coefficient X	1 dB

Space dimension setups (Number of nodes: 5000)					
'Cube'		'Uneven'		'Tube'	
$1 \times 1 \times 1$ cm		$3 \times 1 \times \frac{1}{3}$ cm		$4 \times \frac{1}{2} \times \frac{1}{2}$ cm	

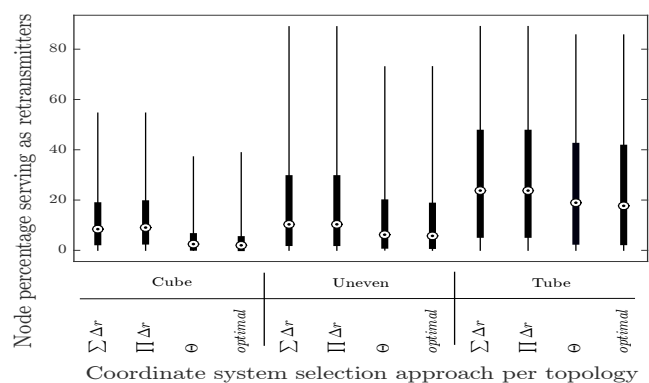


Figure 4. The effects of coordinate system selection (anchor triplet) approach on the number of retransmitters.

involved in each pairwise node communication. The “cube” offers the lowest average numbers, followed by “uneven” and “tube”. Cubic spaces make more room for well-defined, non-cropped volumes of retransmitters near their center, as shown in Fig. 2a. When one (“uneven”) or two (“cube”) space dimensions become significantly smaller than the rest, the volume generally fills the complete dimension range, and is cropped by the corresponding boundaries. Thus, in terms of ratio, the resulting volume fills a good part of the total space.

Regarding the efficiency of the coordinate system selection, it is observed that the Θ -approach provides the best results over all cases, essentially coinciding with the *optimal* in all cases. Nonetheless, the $\Pi \Delta r$ and $\Sigma \Delta r$ approaches also offer decent performance, yielding just 5% more retransmitters than *optimal* on average. However, their deviation is higher, especially in cubic spaces. Thus, the proper choice among the compared approaches depends on the space dimensions, the processing capabilities of the nanonodes (integer/floating point processing) and the total number of nodes in the network. Small networks (e.g., $\propto 10^3$ nodes) may see little absolute difference with a 5% decrease in retransmitters, compared to large networks (e.g., $\propto 10^6$ nodes).

Evaluation of resilience against failures. The nodes are placed in the “cube” space. The “uneven” and “tube” cases

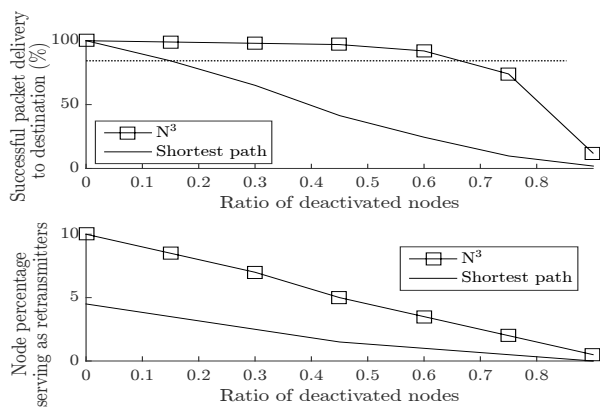


Figure 5. Resilience against node failures for the proposed N^3 and the shortest path routing approach.

produce similar results and are omitted. Prior to each simulation run, we forcibly deactivate a random percentage of the nodes, mimicking failures. Then, 100 powered node pairs are sequentially selected to attempt a packet deliver. The N^3 routing is compared to the shortest path approach, which deduces the packet route using Bresenham's line algorithm [18]. This algorithm requires integer computations only, while each retransmitter is also picked by a Boolean condition (albeit more complex than (1)). Thus, we use the $\sum \Delta r$ approach with N^3 , which also meets these specifications. We log the percentage of successfully delivered packets (out of 100) and the average number of retransmitters involved (out of the total 5000). All runs are repeated for 95% confidence and the resulting average values are given in Fig. 5.

The proposed N^3 allows the network to remain operational in considerably challenging conditions, as shown in the top inset of Fig. 5. Specifically, the network is able to deliver packets with a success rate of 80%, even when 70% of the nodes have gone offline. On the other hand, the shortest path routing drops to the same success rate when just 15% of the nodes have deactivated. Regarding the average number of involved retransmitters, N^3 requires two times as many as the shortest path routing (bottom inset, Fig. 5). This relative difference remains constant for any ratio of deactivated nodes.

The shortest path routing is representative of related approaches aiming at the minimization of energy expenditure at network level. Due to the early research focus on possible solutions to the nanonode power supply, energy efficiency has constituted a primary concern for nano-routing solutions [5]. When considering mission critical applications, information resiliency is the utmost concern, even in the presence of (considerable) changing conditions, such as failing or 'sleepy' nodes. For example, failed data delivery within smart materials means bad adaptation to environmental conditions. Thus, as the presented results show, focusing on energy conservation alone may negate the primary role of a network, which is the delivery of information in a wide range of operating conditions. The proposed N^3 routing scheme is an initial

step towards nano-routing schemes that take energy efficiency into account, however, without undermining the efficiency of networking.

VI. CONCLUSION

The present paper introduced the N^3 , an addressing and routing scheme for 3D nanonetworks. N^3 addresses each node by its distances from a selected set of anchor points. These distances also define volumes through which packets are routed via multi-hop retransmissions. Thus, N^3 naturally provides path multiplicity and node failover, which are mandatory in the challenging nano-environment. N^3 was optimized analytically in terms of minimization of retransmissions, whilst ensuring the high resilience of the network demanded by SDMs and their future applications in various field, e.g. in industrial materials and highly efficient renewable energy sources. Evaluation via realistic simulations in challenging network conditions yielded robust data delivery compared to shortest-path routing approaches.

REFERENCES

- [1] C. Liaskos *et al.*, "Building Software Defined Materials with Nanonetworks," *IEEE Circuits and Systems Magaz.*, vol. 15, no. 4, pp. 12–25, 2015.
- [2] J. Jornet and I. Akyildiz, "Joint Energy Harvesting and Communication Analysis for Perpetual Wireless Nanosensor Networks in the Terahertz Band," *IEEE Trans. on Nanotech.*, vol. 11, no. 3, pp. 570–580, 2012.
- [3] I. Akyildiz and J. Jornet, "The Internet of nano-things," *IEEE Wireless Comm.*, vol. 17, no. 6, pp. 58–63, 2010.
- [4] J. Jornet *et al.*, "PHLAME: A Physical Layer Aware MAC protocol for Electromagnetic nanonetworks in the Terahertz Band," *Nano Communication Networks*, vol. 3, no. 1, pp. 74–81, 2012.
- [5] S. Mohrehkesh and M. Weigle, "RIH-MAC: Receiver-Initiated Harvesting-aware MAC for NanoNetworks," in *ACM ICNCC'14*. ACM, 2014, pp. 180–188.
- [6] G. Piro, G. Boggia, and L. Grieco, "On the design of an energy-harvesting protocol stack for Body Area Nano-NETworks," *Nano Comm. Networks*, vol. 6, no. 2, pp. 74–84, 2015.
- [7] M. Younis *et al.*, "Topology management techniques for tolerating node failures in wireless sensor networks: A survey," *Computer Networks*, vol. 58, pp. 254–283, 2014.
- [8] K. Kantelis *et al.*, "On the Use of FDTD and Ray-Tracing Schemes in the Nanonetwork Environment," *IEEE Comm. Letters*, vol. 18, no. 10, pp. 1823–1826, 2014.
- [9] C. Liaskos and A. Tsioliaridou, "A Promise of Realizable, Ultra-Scalable Communications at nano-Scale: A multi-Modal nano-Machine Architecture," *IEEE Trans. on Comp.*, vol. 64, pp. 1282–1295, 2015.
- [10] A. Tsioliaridou *et al.*, "Lightweight, self-tuning data dissemination for dense nanonetworks," *Nano Comm. Networks*, (In Press), 2015.
- [11] —, "CORONA: A Coordinate and Routing system for Nanonetworks," in *ACM NANOCOM'15*, 2015, pp. 18:1–18:6.
- [12] K. Gibson and H. Scheraga, "Volume of the intersection of three spheres of unequal size: a simplified formula," *The Journal of Physical Chemistry*, vol. 91, no. 15, pp. 4121–4122, 1987.
- [13] XJ Technologies, "The AnyLogic Simulator," 2013. [Online]. Available: <http://www.xjtek.com/anylogic/>
- [14] ITU-R, "Rec. P.676-7: Attenuation by atmospheric gases," Feb. 2007.
- [15] J. Jornet and I. Akyildiz, "Channel Modeling and Capacity Analysis for Electromagnetic Wireless Nanonetworks in the THz Band," *IEEE Trans. on Wireless Comm.*, vol. 10, no. 10, pp. 3211–3221, 2011.
- [16] S. Kim and A. Zajic, "A path loss model for 300-GHz wireless channels," in *IEEE ISAP'14*, 2014, pp. 1175–1176.
- [17] A. Iyer, C. Rosenberg, and A. Karnik, "What is the right model for wireless channel interference?" *IEEE Trans. on Wireless Comm.*, vol. 8, no. 5, pp. 2662–2671, 2009.
- [18] S. Ferguson, *Practical algorithms for 3D computer graphics*, 2nd ed., 2013.